and angiogenesis (27). Overexpression of Akt isoforms has been reported in several cancers (28-30). In androgen-independent LNCaP cells, Akt activity was increased and diminished p27 expression was seen, compared to the androgen-dependent LNCaP (31).

The present study was undertaken to investigate the mechanisms by which PA induces p27 expression in human prostate cancer cells. We noted that PA modulates p27 expression mainly by post-translational regulation through Skp2 and partly by AKT-mediated transcriptional regulation.

Materials and Methods

Materials. Phenylacetate (PA) was purchased from Wako LIFE Science (Osaka, Japan). Antibody against p27 was obtained from Transduction Laboratories (Lexington, KY, USA), against Skp2 from Zymed Laboratories (San Francisco, CA, USA) and against Akt and phospho-Akt from New England Biolabs (Beverly, MA, USA). [α-^{32}P]dCTP was purchased from Amersham Biosciences (Piscataway, NJ, USA).

Cell culture. The human prostate cancer cell lines LNCaP and PC-3 were purchased from the American Type Culture Collection (ATCC, Rockville, MD, USA) and cultured in RPMI-1640 (LNCaP) or DMEM/F12 (PC-3) medium supplemented with 10% fetal bovine serum (FBS), penicillin (100U/ml) and streptomycin (100μ/ml), in a water-jacketed incubator with a humidified atmosphere (5%CO_2, 95% air) at 37°C. AIDL (androgen-independent LNCaP cells), which can grow very well in the absence of androgen, was induced by being maintained in phenol red-free RPMI-1640 medium with 2% charcoal-stripped FBS for over 2 years, as described previously (13). Experimental cultures were grown to 60-70% confluency and then treated with 5 mM PA or vehicle (ethanol) by replacing the medium supplemented with 10% FBS and either PA or ethanol. The amount of ethanol added as the vehicle never exceeded 0.1% of the total volume.

Western blot analysis. Cells were rinsed twice with ice-cold PBS and lysed in 1 ml of NP-40 lysis buffer: 50 mM Tris-HCl[pH 7.4], 150 mM NaCl, 10 mM NaF, 5 mM EDTA, 2 mM sodium vanadate, 0.5% sodium deoxycholate 1 mM DTT, 1 mM phenylmethylsulfonyl fluoride (PMSF), 2 μg/ml aprotinin and 0.1% NP-40. Protein concentrations were measured at least twice by Bio-Rad protein assay reagent (Bio-Rad, Hercules, CA, USA). For Western blot analysis, protein samples were boiled for 5 minutes in Laemmli buffer and separated on 6-12% SDS-polyacrylamide gel electrophoresis (SDS-PAGE). The gels were then transferred to nitrocellulose membrane (Hybond ECL, Amersham Biosciences) by a semi-dry transfer method. The transferred membranes were soaked in Ponseau-S solution (Sigma, St. Louis, MO, USA) to check for comparable amounts of proteins loaded and the homogeneity of transfer. After blocking with TBST-MILK (Tris-buffered saline[pH7.4], 0.1% tween 20, 5% low fat milk), the membrane for p27 was incubated with primary antibody (1:2500) for 1-2 hours in TBST-MILK and membranes for Akt and Skp2 (1: 1000) in TBST-BSA (TBST containing 5% BSA). Then the membranes were incubated with secondary antibody conjugated with HRP for 1 hour, before developing with the enhanced chemiluminescence (ECL) detection system (PIERCE, Rockford, USA).

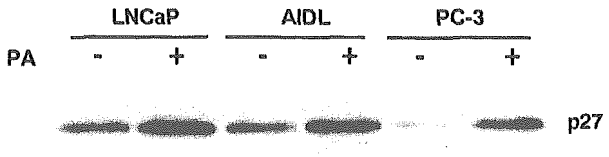

Figure 1. *Effect of PA on p27 protein expression in LNCaP, AIDL and PC-3 cells. Cells were treated with 5mM PA for 24 hours. Fifty μg of total cell lysates were subjected to immunoblot analysis with p27 antibody.*

Northern blot analysis. Total RNA was extracted from growing cells using ISOGEN (Waco Pure Chemical Industries , Osaka, Japan). Electrophoresis was performed on 1.2% agarose-formaldehyde gel (sample 15 μg) and the gels were transferred to Hybond NX nylon membranes (Amersham Biosciences) in 20XSSC (3 M NaCl, 8 mM NaOH, 2 mM sarkosy) and were fixed by UV crosslinker. DNA fragments for p27 and Skp2 were amplified by PCR as previously described (29), and radiolabelled using Prime-a-Gene Labeling System (Promega, Madison, WI, USA). Membranes were prehybridized and hybridized with [α-^{32}P]dCTP-labelled probes in Hybridization Solution (Nacalai Tesque, Kyoto, Japan). After hybridization, the membranes were washed in 2XSSC at 68°C twice and 1XSSC at 68°C twice. Autoradiography was performed using Amersham ECL X-ray film at –70°C with an intensifying screen.

Real-time PCR. Total RNA was extracted as described above. After reverse-transcription, Real-time PCR was performed using an ABI PRISM 7700 Sequence Detection System instrument and software (PE Applied Biosystems, Foster City, CA, USA). The reaction mix contained cDNA template, PCR Master Mix (PE Applied Biosystems) and Assays-on-demand™ Gene Expression Products (PE Applied Biosystems) in total 50 μl for mRNA analysis of p27, Skp2 and 18S. For Cks1 mRNA analysis, primers were as follows: 5'-GGTCCATTATATGATCCATGAACCG-3', 3'-GAAAAGTCGGAGTTCGAAATGTGT-5', and probe was FAM-TTCCGGCACCCACTACCCGAGAA-TAMRA.

Ubiquitination assay. We used the Ubiquitinated Protein Enrichment Kit obtained from Calbiochem(La Jolla, CA, USA & Canada). Forty μl of polyubiquitin affinity beads were added to 2 mg of cell lysate and lysis buffer(50 mM HEPES[pH7.5], 5 mM EDTA, 150 mM NaCl and 1% Triton X-100) with protease inhibitor cocktail and 10 mM N-ethylmaleimide was added to a total volume of 1 ml, followed by incubation at 4°C for 3 hours. After centrifugation for 5 seconds at 4°C, the supernatant was removed and washed in 1 ml lysis buffer. The beads were suspended in 2X gel loading buffer(250 mM Tris-HCl[pH6.8], 4% SDS, 10% β-mercaptoethanol, 20% glycerol, bromophenol blue), and boiled for 5 minutes. After centrifugation for 1 minute at 13,700 xg, the lysates were separated on 8% SDS-polyacrylamide gel electrophoresis. Then the gel was transferred to Hybond ECL nylon membranes (Amersham Biosciences). After washing, blocking was performed for 1 hour. The membrane was incubated with primary antibody (p27, 1:1000) for 1-2 hours in blocking buffer and then the membranes were incubated with secondary antibody conjugated with HRP (IgG mouse, 1: 2500). Developing with ECL advance (Amersham Biosciences) autoradiography was performed. All experiments were performed in triplicate unless otherwise specified.

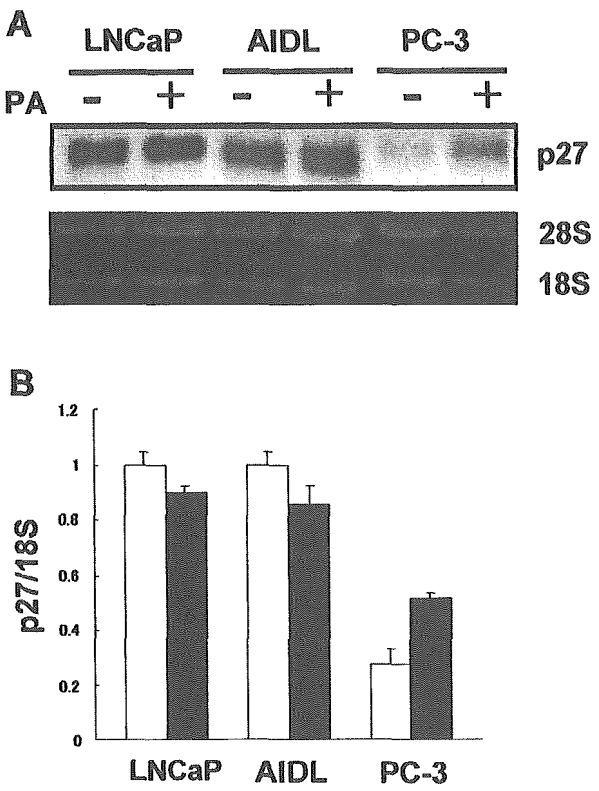

Figure 2. *Effect of PA on p27 mRNA expression. Total cellular RNA was extracted from LNCaP, AIDL and PC-3 cells after PA treatment for 24 hours. (A) Fifty μg of total RNAs were used for Northern blot analysis. (B) Expression of p27 mRNA was analyzed using quantitative real-time RT-PCR. Fold increase of mRNA in PA-treated cells were calculated comparing with eukaryotic 18S as an internal standard. About a two-fold increase was observed in PC-3 cells, although a significant increase was not demonstrated in LNCaP and AIDL cells. Open squares show control cells, and closed squares indicate PA-treated cells.*

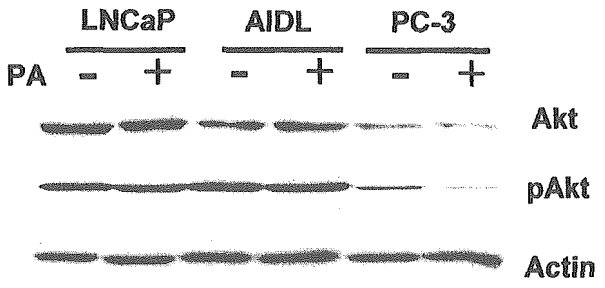

Figure 3. *Effect of PA on Akt and phospho-Akt (Ser-473) protein levels following PA treatment. Akt and p-Akt protein levels were determined by immunoblot analysis with Akt and phospho-Akt antibodies (using 50μg of cell lysates).*

Results

Effect of phenylacetate on p27 in prostate cancer cells. It is well known that PA induces a perturbation of the cell cycle progression, especially G1 arrest. Our previous report showed that PA concentrations in the range of 4-6 mM have antiproliferative effects in prostate cancer cells and that p27 is a key target in this process (13). We used the well-known LNCaP (androgen-dependent), PC-3 (androgen-independent) and an androgen-independent LNCaP (AIDL) cell line, which was isolated in our laboratory as described previously (13). In this study, cells were cultured in serum containing medium with 5 mM concentrations of PA for 24 hours, and proteins were extracted from these cells as described in Materials and Methods. We first examined the protein levels of p27. Western blot analysis showed that p27 protein levels were increased in PA-treated cells. Interestingly, p27 basal expression in PC-3 cells was lower than LNCaP and AIDL, suggesting that a more malignant state is associated with a lower level of p27 (Figure 1).

Next, to determine whether the increase in p27 was regulated transcriptionally, Northern blot analysis was performed. p27 expression did not change significantly in LNCaP and AIDL, however PC-3 cells exhibited very low basal levels of p27 mRNA, which was greatly elevated after PA addition (Figure 2A). The change of p27 mRNA expression was also analyzed by real-time RT-PCR. PC-3-treated cells demonstrated an increase of approximately 2-fold over control cells. The same as the results of Northern blot, LNCaP and AIDL cells did not show any remarkable changes (Figure 2B). These data suggest that PA-induced p27 expression might be regulated at the translational level in LNCaP and AIDL.

Akt activity in PA-treated prostate cancer cells. It has been reported that Akt may enhance cell cycle progression by diminishing expression of p27 (31). To assess the effect of PA on Akt expression and activation, total cell lysates from PA-treated cells were analyzed by Western blot. Although Akt expression levels were unchanged (Figure 3), Akt activation (Ser-473 phosphorylation) was markedly decreased in PC-3 cells compared to LNCaP and AIDL. The down-regulation of AKT activity (measured by Ser-473 phosphorylation) by PA could be one of the mechanisms of diminishing p27 expression in PC-3 cells. These data suggest that some mechanism other than the Akt pathway may be implicated in p27-regulation by PA in LNCaP and AIDL.

PA treatment down-regulates Skp2 expression in prostate cancer cells. Recent evidence has strongly suggested that the intracellular concentration of p27 is predominantly regulated by Skp2, an F-box protein, through the ubiquitin-proteasome proteolityc pathway (19, 20). Thus, to further characterize the involvement of this pathway in PA-treated

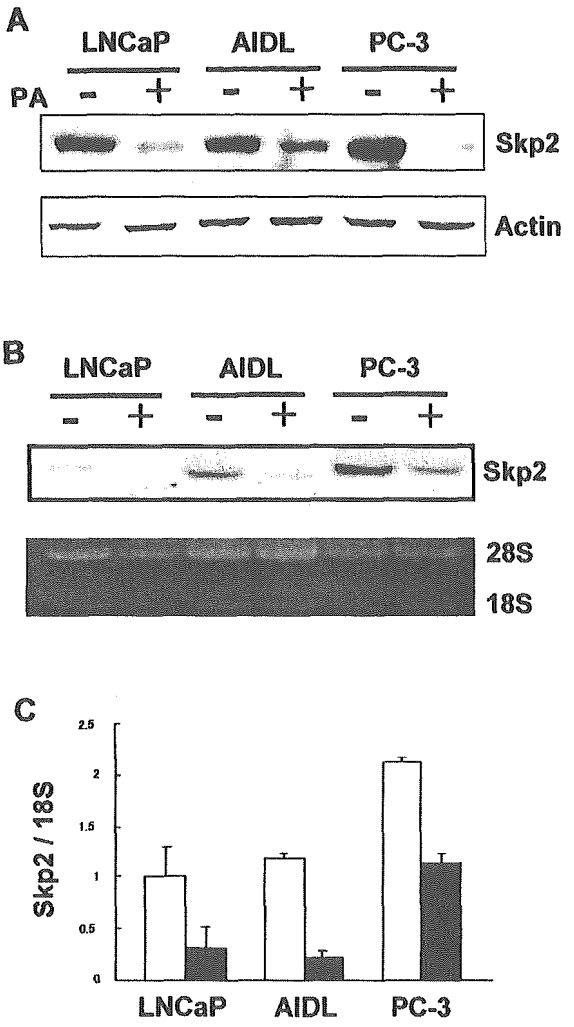

Figure 4. *Expressions of Skp2 protein and mRNA levels after PA treatment. (A) After 5 mM PA treatment, protein levels were examined by immunoblot analysis with Skp2 antibody. (B) Northern blot analysis showed a substantial decrease of Skp2 mRNAs in all three PA-treated cells. (C) Skp2 mRNA levels were determined using real-time RT-PCR. Compared with eukaryotic 18S mRNA level, each mRNA level of control and PA-treated cells was estimated.*

cells, we examined the expression of Skp2 by immunoblot analysis. Basal Skp2 expression was higher in PC-3 cells relative to LNCaP and AIDL cell lines. Skp2 expression decreased in PA-treated cells after 24 hours. This decrease was more pronounced in PC-3 cells (Figure 4A). Skp2 mRNA levels were also assessed by Northern blot and real-time PCR. Northern blot analysis showed a drastical decrease in Skp2 mRNA (Figure 4B). Quantitation by real-time PCR also showed a diminished expression, about 80% in LNCaP and AIDL cells, and more than 40% in PC-3 cells (Figure 4C). Evidence that Cks1 is essential for ubiquitin ligation of p27 and that it greatly enhanced the binding of

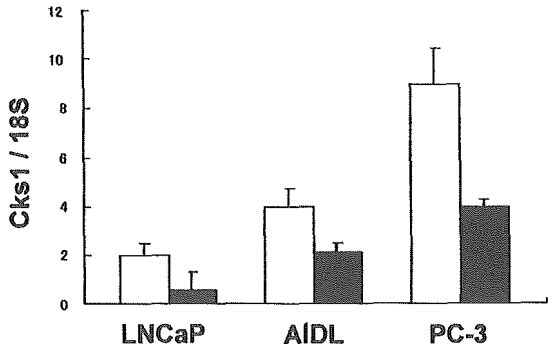

Figure 5. *mRNA expressions of Cks1 in PA-treated and untreated prostate cancer cells. Real-time RT-PCR analysis shows a clear decrease after 5 mM PA treatment (compared with eukaryotic 18S mRNA level). Open squares show control cells, and closed squares indicate PA-treated cells.*

T187-phosphorylated p27 has been reported (21). To investigate the role of Cks1 in these effects, real-time PCR was undertaken. Cks1 mRNA expression was higher in PC-3 cells than LNCaP and AIDL cells. A decreased Cks1 expression was noted after PA addition in all the cell lines. This decreased expression was in the range of approximately 50% to 75% being higher for LNCaP and lower for AIDL and PC-3 cells (Figure 5). These data suggest that Skp2 and Cks1 expression are modulated by PA and might be involved in p27 regulation.

PA-induced p27 up-regulation correlates with decreased p27 ubiquitination. Real-time PCR revealed that PA-induced Skp2 down-regulation at the protein level mirrors changes in the mRNA state in the studied cell lines. In contrast, p27 mRNA levels were up-regulated only in PC-3 cells, but were unchanged in LNCaP and AIDL cells. These results indicate that the effect of PA on p27 mRNA levels could not fully account for the accumulation of p27 protein, especially in the androgen-independent/sensitive AIDL and its parental androgen-dependent LNCaP cells. Thus, we hypothesize that p27 up-regulation in response to PA may be mediated by alterations in p27 protein stability. To confirm this hypothesis , we performed an *in vitro* ubiquitination assay. p27 ubiquitination, represented by a ladder-type pattern following PA addition, was diminished after 24-hour treatment in all three cell lines (Figure 6). A previously described non-specific band at about 60 kD was seen, probably a crossreacting protein (21). These data may indicate that PA decreases p27-ubiquitin ligation and further degradation by diminishing Skp2 activity in prostate cancer cell lines.

Discussion

Although androgen withdrawal is the most effective therapy for patients with advanced prostate cancer, progression to

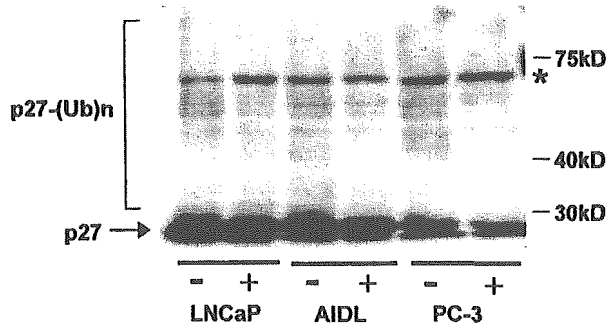

Figure 6. *In vitro ubiquitination of p27. Two mg proteins of whole cell lysates were incubated with ubiquitin affinity beads for 4 hours and the precipitates were subjected to SDS-PAGE, immunoblotted with p27 antibody. Ubiquitinated p27 was decreased in 5 mM PA-treated prostate cancer cells. Asterisk shows non specific bands at about 60 kD.*

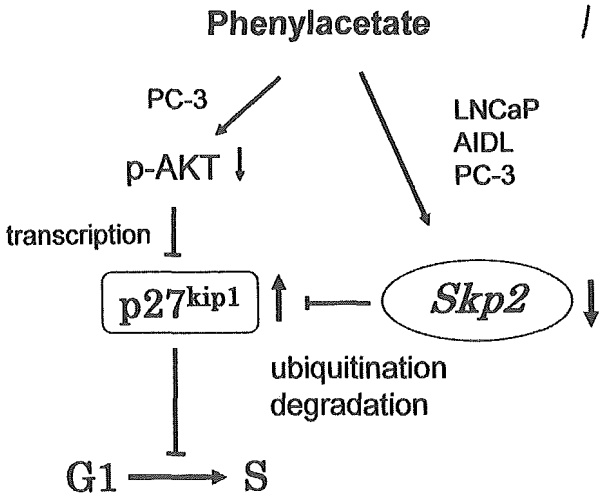

Figure 7. *Proposed model for the pathway of phenylacetate-mediated G1 arrest through p27 in prostate cancer cells. PA decreases Skp2 expression in three prostate cancer cell lines, and phosph-AKT (p-AKT) is down-regulated by PA in only PC-3 cells. Thus, p27 is up-regulated post-translationally in three prostate cell lines, and both transcriptionally and post-translationally in PC-3 cells, followed by G1 arrest.*

androgen independence eventually occurs and remains the main barrier to improved survival and quality of life. Traditional treatment with cytotoxic chemicals is usually ineffective because of low proliferation rates and is limited by toxicity (2). Progression to androgen independence is an intricate process, involving clonal selection and adaptative mechanisms in heterogeneous tumors composed of subpopulations of cells that behave differently to androgen ablation. Thus, it is possible to manipulate these changes triggered by androgen ablation through the adjuvant use of differentiation agents or by modulating the expression of genes involved in the process.

Phenylacetate (PA) has been identified as having antiproliferative effects against several malignant cell types (9-12), however, the molecular mechanism by which PA induces its differentiation and cell cycle arrest has not been elucidated. Our previous report demonstrated the involvement of p27 in PA-mediated cell cycle arrest in prostate cancer cells (13). In the present study, we investigated the mechanism by which PA increased p27 expression in prostate cancer cells. It was reported that Akt activity is associated with transcriptional regulation of p27 in LNCaP (31), however, in this study PA had no effect on p27 mRNA as well as Akt and phospho-Akt, suggesting that PA has little effect on p27 transcription in LNCaP and AIDL cells. Therefore, stabilization in the p27 protein could be responsible for the intracellular accumulation of p27 in PA-treated LNCaP and AIDL cells. Recent reports have strongly suggested that the intracellular concentration of p27 is regulated predominantly by Skp2, an F-box protein, through the ubiquitin-proteasome proteolytic pathway (19, 20). Thus, we hypothesized that the PA-mediated increase in p27 expression could result from the ligand-dependent decrease in Skp2. Our data demonstrated that PA decreased both Skp2 and Cks1 expressions, and p27 ubiquitination. These results suggest that PA decreases p27-ubiquitin ligation and further degradation by diminising Skp2 activity in prostate cancer cells. We believe that PA-induced cell cycle arrest is correlated with inhibition of Skp2-mediated proteolytic degradation of p27 (Figure 7).

The PTEN (phosphatase and tensin homolog deleted in chromosome ten)/MMAC (mutated in multiple advanced cancers) is a tumor suppressor gene associated with multiple tumors, including prostate cancer (32-36). Loss of PTEN/MMAC function can occur through homozygous gene deletion, point mutation, or loss of expression (35). Previous reports have demonstrated that PTEN is mutated in LNCaP and PC-3 cells (37). PTEN negatively regulates the phosphorylation of Akt and increases p27 expression, resulting in the inhibition of the transition from G1- to S-phase of the cell cycle (31, 37). In mouse embryonic stem cells, PTEN increases the p27 protein level and down-regulates the mRNA level of Skp2, but has little effect on transcriptional regulation of p27 and other components of SCF^{skp2} (38). Our results demonstrated that not only p27 mRNA, but also Akt protein and phospho-Akt levels did not change in LNCaP and AIDL, indicating that PA has little effect on transcriptional levels of p27 in these prostate cancer cells. Interestingly, PA increased p27 mRNA levels and decreased Akt phosphorylation in PC-3 cells. These data suggest that PA has effects on the transcriptional

regulation of p27 as well as post-translational regulation in PC-3 cells (Figure 7). Differences in the effect of PA can be related to the androgen-independent status and/or cancer progression. The Akt pathway may play an additive role in the regulation of p27 expression during prostate cancer progression.

Other antiproliferative effects of PA have been reported to be correlated with the peroxisome proliferator-activated receptor γ (PPARγ), which is a member of the nuclear receptor family (39, 40). PPARγ ligands have demonstrated a growth-inhibitory effect on several malignant cell types, including prostate cancer (41-43). PA increases PPARγ expression, interacts directly with the ligand-binding site of PPARγ and activates its transcriptional function in human breast carcinoma and glioblastoma cells (44). PA inhibited cell proliferation and induced differentiation in human neuroblastoma cells through the PPARγ signaling pathway (45). These findings provide evidence for a biological role of PPARγ in tumor cytostasis induced by PA. A decrease in Skp2 expression and a reciprocal increase in p27 expression were found in PPARγ ligand, troglitazone-treated hepatoma cells (43). Thus, it might be one of the candidates of downstream target molecules of PA, although we did not examine whether PA has any effect on PPARγ expressions in prostate cancer cells.

Skp2 is considered to be a protooncogene, and is overexpressed in several human cancers (46-48). Expression of Skp2 alone is sufficient to reduce p27 levels and induce hyperplasia, dysplasia and low-grade carcinomas in the mouse prostate gland in transgenic mouse lines that specifically expressed Skp2 (49). Skp2 is inversely correlated with p27 and a significant correlation was found between Skp2 levels and tumor aggressiveness in prostate cancer (48). Ours and other studies collectively suggest that PA could be a useful therapeutic compound for both androgen-dependent prostate cancer, preventing the hormone-refractory state induced by hormone depletion therapy, and hormone-refractory prostate cancer. In the present study, profound down-regulation of Skp2 and a reciprocal increase of p27 by PA were observed in the more aggressive androgen-independent prostate cancer cell line, PC-3. Thus, a strategy of targeting Skp2 may provide a more selective target for the treatment of advanced prostate cancer.

Acknowledgements

We thank Dr. H. Koga for technical advice on *in vitro* ubiquitination of p27 and Dr. M. Takeo for technical asistance with real-time RT-PCR.

This work was supported in part by a Grant-in-Aid from the Ministry of Education, Science and Culture of Japan (90179151 and 10175995) and the Ministry of Health, Labor and Welfare of Japan (H13-013).

References

1 Huggins C and Hodges CV: Studies on prostate cancer. I. The effect of castration, of estrogen, and androgen injection on serum phosphatases in metastatic carcinoma of the prostate. Cancer Res *1*: 293, 1941.

2 Glitters RF: Carcinoma of the prostate. N Engl J Med *324*: 235-245, 1991.

3 Sndler M, Ruthven CR, Goodwin BL, Lees A and Stern GM: Phenylacetic acid in human body fluids: high correlation between plasma and cerebrospinal fluid concentration values. J Neurol Neurosurg Psychiatry *45*: 366-368, 1982.

4 Brusilow SW, Danney M, Waber LJ, Batshaw M, Burton B, Levitsky L, Roth K, McKeethren C and Ward J: Treatment of episodic hyperammonemia in children with inborn errors of urea synthesis. N Engl J Med *310*: 1630-1634, 1984.

5 del Rosario M, Werlin SL and Lauer SJ: Hyperammonemic encephalopathy after chemotherapy. Survival after treatment with sodium benzoate and sodium phenylacetate. J Clin Gastroenterol *25*: 682-684, 1997.

6 Samid D, Yeh A and Prasanna P: Induction of erythroid differentiation and fetal hemoglobin production in human leukemic cells treated with phenylacetate. Blood *80*: 1576-1581, 1992.

7 Samid D, Shack S and Sherman LT: Phenlyacetate: a novel nontoxic inducer of tumor cell differentiation. Cancer Res *52*: 1988-1992, 1992.

8 Samid D, Shack S and Myers CE: Selective growth arrest and phenotypic reversion of prostate cancer cells *in vitro* by nontoxic pharmacological concentrations of phenylacetate. J Clin Invest *91*: 2288-2295, 1993.

9 Cinatl JJ, Cinatl J, Mainke M, Weibflog A, Rabenau H, Kornmhuber B and Doerr HW: *In vitro* differentiation of human neuroblastoma cells induced by sodium phenylacetate. Cancer Lett *70*: 41-48, 1993.

10 Shack S, Miller A, Liu L, Prasanna P, Thibault A and Samid D: Vulnerability of multidrug-resistant tumor cells to the aromatic fatty acids phenylacetate and phenylbutyrate. Cancer Res *2*: 865-872, 1996.

11 Gore SD, Samid D and Weng LJ: Impact of the putative differentiationing agents sodium phenylbutyrate and sodium phenylacetate on proliferation, differentiation and apoptosis of primary neoplastic myeloid cells. Clin Cancer Res *3*: 1755-1762, 1997.

12 Omar E, Onishi T, Umeda Y, Soga N, Wakita T, Arima K, Yanagawa M and Sugimura Y: Phenylacetate inhibits growth and modulates cell cycle gene expression in renal cancer cell lines. Anticancer Res *23*: 1637-1642, 2003.

13 Onishi T, Yamakawa K, Omar E, Suzuki R and Kawamura J: p27kip1 is the key mediator of phenylacetate induced cell cycle arrest in human prostate cancer cells. Anticancer Res 20: 3075-3082, 2000.

14 Yang RM, Naitoh J, Murphy M, Wang H-J, Phillipson J, DEKernion JB, Loda M and Reiter RE: Low p27 expression predicts poor disease-free survival in patients with prostate cancer. J Urol *159*: 941-945, 1998.

15 Barnes A, Pinder SE, Bell JA, Paish EC, Wencyk PM, Robertson JFR, Elston CW and Ellis IO: Expression of p27kip1 in breast cancer and its prognotic significance. J Pathol *201*: 451-459, 2003.

16 Filipits M, Pohl G, Stranzl T, Kaufmann H, Jutta A, Gisslinger H, Greinix H, Chott A and Drach J: Low p27kip1 expression is an independent adverse prognostic factor in patients with multiple myeloma. Clin Cancer Res *9*: 820-826, 2003.
17 Nitti D, Belluco C, Mammano E, Marchet A, Ambrosi A, Mencarelli R, Segato P and Lise M: Low levels of p27kip1 protein expression in gastric adenocarcinoma is associated with disease progression and poor outcome. J Surg Oncol *81*: 167-176, 2002.
18 Armengol C, Boix L, Bachs O, Sole M, Fuster J, Sala M, Llovet JM, Rodes J and Bruix J: p27kip1 is an independent predictor of recurrence after surgical resection in patients with small hepatocellular carcinoma. J Hepatol *38*: 591-597, 2003.
19 Nakayama K-I, Hatakeyama S and Nakayama K: Regulation of the cell cycle at the G1-S transition by proteolysis of cyclin E and p27kip1. Biochem Biophys Res *282*: 853-860, 2001.
20 Carrano AC, Eytan E, Hershko A and Pagano M: SKP2 is required for ubiquitin-mediated degradation of CDK inhibitor p27. Nature Cell Biol *1*: 193-199, 1999.
21 Ganoth D, Bornstein G, Ko TK, Larsen B, Tyers M, Pagano M and Hershko A: The cell cycle regulatory protein Cks1 is required for SCFSkp2-mediated ubiquitinylation of p27. Nature Cell Biol *3*: 321-324, 2001.
22 Medema RH, Kops GJ, Bos JL and Burgering BMT: AFX-like Forkhead transcription factors mediate cell-cycle regulation by Ras and PKB through p27kip1. Nature *404*: 782-787, 2000.
23 Brunet A, Bonni A, Zigmond MJ, Lin MZ, Juo P, Hu LS, Anderson MJ, Arden KC, Blenis J and Greenberg M: Akt promotes cell survival by phosphorylating and inhibiting a Forkhead transcription factor. Cell *96*: 857-858, 1999.
24 Kops GJ, Ruiter NDd, Vries-Smits AMd, Powell DR, Bos JL and Burgering BM: Direct control of the Forkhead transcription factor AFX by protein kinase B. Nature *398*: 630-634, 1999.
25 Tang ED, Nunez G, Barr FG and Guan KL: Negative regulation of the Forkhead transcription factor FKHR by Akt. J Biol Chem *274*: 16741-16746, 1999.
26 Takaishi H, Konishi H, Matsuzaki H, Ono Y, Shirai Y, Saiti N, Kitamura T, Ogawa W, Kasuga M, Kikkawa U and Nishizuka Y: Regulator of nuclear translocation of Forkhead transcription factor AFX by protein kinase B. Proc Natl Acad Sci USA *96*: 11836-11841, 1999.
27 Hill MM and Hemmings BA: Inhibition of protein kinase B/Akt: implications for cancer thrapy. Pharmacol Ther *93*: 243-251, 2002.
28 Nakatani K, Thompson DA, Barthel A, Sakaue H, Liu W, Weigel RJ and Roth RA: Up-regulation of Akt3 in estrogen receptor-deficient breast cancers and androgen-independent prostate cancer lines. J Biol Chem *274*: 21528-21532, 1999.
29 Cheng JQ, Ruggeri B, Klein WM, Sonoda G, Altomare DA, Watson DK and Testa J: Amplication of AKT2 in human pancreatic cells and inhibition of AKT2 expression and tumorigenicity by antisense RNA. Proc Natl Acad Sci USA *93*: 3636-3641, 1996.
30 Bellacosa A, Feo Dd, Godwin AK, Bell DW, Cheng JQ, Altomare DA, Wan M, Dubeau L, Scambia G, Masciullo V, Ferrandina G, Benedetti-Panici P, Mascuso S, Neri G and Testa J: Molecular alterations of the AKT2 oncogene in ovarian and breast carcinomas. Int J Cancer *64*: 280-285, 1995.
31 Graff J, Konicek BW, McNulty AM, Wang Z, Houck K, Allen S, Paul JD, Hbaiu A, Goode RG, Sandusky GE, Vessella RL and Neubauer BL: Increased AKT activity contributes to prostate cancer progression by dramatically accelerating prostate tumor growth and diminishing p27kip1 expression. J Biol Chem *275*: 24500-24505, 2000.
32 Crirns P, Okami K, Halachmi S, Halachmi N, Esteller M, Herman JG, Jen J, Isaacs WB, Bova GS and Sidransky D: Frequent inactivation of PTEN/MMAC1 in primary prostate cancer. Cancer Res *57*: 4997-5000, 1997.
33 Suzuki H, Freije D, Nusskern DR, Okami K, Cairns P, Sidransky D, Isaacs WB and Bova GS: Interfocal heterogeneity of PTEN/MMAC1 gene alterations in multiple metastatic prostate cancer tissues. Cancer Res *57*: 3660-3663, 1998.
34 Guldberg P, Straten Pt, Birck A, Ahrenkiel V, Lirkin AF and Zeuthen J: Disruption oh the MMAC1/PTEN gene by deletion or mutation is a frequent event in malignant melanoma. Cancer Res *57*: 3660-3663, 1997.
35 Risinger JI, Hayes AK, Berchuck A and Barrett JC: PTEN/MMAC1 mutations in endometrial cancers. Cancer Res *57*: 4736-4738, 1997.
36 Li J, Yen C, Liaw D, Podsypanina K, Bose S, Wang SI, Puc J, Miliaresis C, Rodgers L, McCombie R, Binger SH, Giovanella BC, Ittmann M, Tycko B, Hibshoosh H, Wigler MH and Parsons R: PTEN, a putative protein tyrosine phosphatase gene mutated in human brain, breast, and prostate cancer. Science *275*: 1943-1947, 1997.
37 Persad S, Attwell S, Gray V, Delcommenne M, Troussard A, Sanghera J and Dedhar S: Inhibition of integrin-linked kinase (ILK) suppresses activation of protein kinase B/Akt and induces cell cycle arrest and apoptosis of PTEN-mutant prostate cancer cells. Proc Natl Acad Sci USA *97*: 3207-3212, 2000.
38 Mamillapalli R, Gavrilova N, Mihaylova VT, Tsvetkov LM, Wu H, Zhang H and Sun H: PTEN regulates the ubiquitin-dependent degradation of the CDK inhibitor p27kip1 through the ubiquitin E3 ligase SCFskp2. Curr Biol *11*: 263-267, 2001.
39 Saltiel AR and Olefsky JM: Thiazolidinediones in the treatment of insulin resistance and typeII diabetes. Diabetes *45*: 1661-1669, 1996.
40 Lehmann JM, Moore LB, Smith-Oliver TA, Wilkinson WO, Wilson TM and Kliewer SA: An antidiabetic thiazoidinedione is a high affinity ligand for peroxisome proliferator-activated receptor g (PPARg). J Biol Chem *270*: 12953-12956, 1995.
41 Mueller E, Sarraf P, Tontonoz P, Evans RM, Martin KJ, Zhang M, Fletcher C, Singer S and Spiegelman BM: Terminal differentiation of human breast cancer through PPARg. Mol Cell *1*: 465-470, 1998.
42 Kubota T, Koshizuka K, Williamson EA, Asou H, Said JW, Holden S, Miyoshi I and Koeffler HP: Ligand for peroxisome proliferator-activated receptor γ (troglitazone) has potent antitumor effects against human prostate cancer both *in vitro* and *in vivo*. Cancer Res *58*: 3344-3352, 1998.
43 Koga H, M.Harada, Ohtubo M, Shishido S, Kumemura H, Hanada S, Taniguchi E, Yamashita K, Kumashiro R, Ueno T and Sata M: Troglitazone induces p27kip1-associated cell-cycle arrest through down-regulating Skp2 in human hepatoma cells. Hepatology *37*: 1086-1096, 2003.

44 Samid D, Wells M, Greene ME, Shen W, Palmer CAN and Thibault A: Peroxisome proliferator-activated receptor γ as a novel target in cancer therapy: binding and activation by an aromatic fatty acid with clinical antitumor activity. Clin Cancer Res *6*: 933-941, 2000.

45 Han S, Wada RK and Sidell N: Differentiation of human neuroblastoma by phenylacetate is mediated by peroxisome proliferator-activated receptor γ. Cancer Res *61*: 3998-4002, 2001.

46 Masuda TA, Inoue H, Sonoda H, Mine S, Yoshikawa Y, Nakayama K, Nakayama K and Mori M: Clinical and pathological significance of S-phase kinase-associated protein 2 (Skp2) gene expression in gastric carcinoma; modulation of malignant phenotype by Skp2 overexpression, possibly *via* p27 proteolysis. Cancer Res *62*: 3819-3825, 2002.

47 Schiffer D, Cavalla P, Fiano V, Ghimenti C and Piva R: Inverse relationship between p27/Kip.1 and the F-box protein Skp2 in human astrocytic gliomas by immunohistochemistry and Western blot. Neurosci Lett *328*: 125-128, 2002.

48 Ben-Izhak O, Lahav-Baratz S, Meretyk S, Ben-Eliezer S, Sabo E, Dirnfeld M, Cohen S and Ciechanover A: Inverse relationship between Skp2 ubiquitin ligase and the cyclin dependent kinase inhibitor p27kip1 in prostate cancer. J Urol *170*: 241-245, 2003.

49 Shim EH, Johnson L, Noh HL, Kim YJ, Sun H, Zeiss C and Zhang H: Expession of the F-box protein SKP2 induces hyperplasia, dysplasia, and low-grade carcinoma in the mouse prostate. Cancer Res *63*: 1583-1588, 2003.

Received September 6, 2004
Revised February 1, 2005
Accepted March 4, 2005

The Prostate 65:355–364 (2005)

Natural History of Human Prostate Gland: Morphometric and Histopathological Analysis of Japanese Men

Shinji Fujikawa,[1] Hiroshi Matsuura,[1] Masahiro Kanai,[1] Miki Fumino,[1] Kenichiro Ishii,[1] Kiminobu Arima,[1] Taizo Shiraishi,[2] and Yoshiki Sugimura[1]*

[1]Department of Urology, Mie University Faculty of Medicine, Mie, Japan
[2]Department of 2nd Pathology, Mie University Faculty of Medicine, Mie, Japan

BACKGROUND. To clarify the pathology of the development of prostatic disorders such as inflammation, cancer, and hyperplasia, we compared histopathological findings of the prostate according to age group.

METHODS. Whole-mount sections of prostates were used to assess the relationship between age and prostate weight (n = 962), prostate histological composition in the transition zone (TZ) and in the peripheral zone (PZ) (n = 68), prostate histopathological findings by zone (n = 102), and comparison of latent tumor development by age group (n = 1,815).

RESULTS. A rapid increase in prostate weight from birth to the 20s was followed by a slow rise thereafter. Volume increases ($P < 0.01$) were observed in all components of glandular epithelium, glandular lumen, and stroma in the TZ from the 40s to 70s inclusive. In the PZ, the epithelial and stromal volumes tended to decrease in an age-dependent manner ($P < 0.05$). Calculi and lymphocyte infiltration were detected at a relatively early age, with a tendency towards an age-dependent increase. Glandular dilation and nodular hyperplasia were noted first in the 30s group, also with a tendency towards age-dependent increase. Latent tumors were first detected in the 30s group (5.6%), and slowly increased thereafter.

CONCLUSIONS. There was an age-dependent trend towards prostate glandular dilation and prostate enlargement with inflammation. It was demonstrated that tumor and hyperplasia have a long natural history, usually starting in the fourth decade of life, accompanied by dynamic changes with age in glandular tissue composition as well as cell proliferation activity.
Prostate 65: 355–364, 2005. © 2005 Wiley-Liss, Inc.

KEY WORDS: **natural history; prostate cancer; benign prostatic hyperplasia; morphometric analysis**

INTRODUCTION

The prostate is a unique organ that grows in response to androgenic hormones but that develops, at later age, proliferative lesions such as cancer and hyperplasia, despite decreasing androgen levels with advancing age. Regarding the natural history of the prostate, a study by Berry et al. [1] that reported on age-related changes in prostate weight and in the prevalence of pathological benign prostatic hyperplasia (BPH) is well known and is a frequently cited reference. However, in Asian populations including the Japanese, where the incidence of prostatic hyperplasia and cancer is considered to be low, no such large-scale research has been conducted.

The epidemiological study data accumulated to date have revealed, as an ethnic group-associated risk, that prevalence rates of prostatic hyperplasia and clinical and latent tumors are highest in the black, followed by Caucasian, and then Asian populations.

Grant sponsor: Ministry of Education, Science and Culture of Japan; Grant numbers: 90179151, 10175995; Grant sponsor: Ministry of Health, Labor and Welfare of Japan; Grant number: H13-013.

*Correspondence to: Yoshiki Sugimura, Department of Urology, Mie University Medical School 2-174 Edobashi, Tsu, Mie 514-8507, Japan.
E-mail: sugimura@clin.medic.mie-u.ac.jp

Received 10 September 2004; Accepted 3 November 2004
DOI 10.1002/pros.20208
Published online 21 July 2005 in Wiley InterScience (www.interscience.wiley.com).

However, there is a lack of well-documented relevant data obtained from Japanese subjects, and it is debatable whether the findings by Berry et al. [1], that is, the prostate grows rapidly from birth to the 30s and nodular hyperplasia begins to develop commonly in the 30s, with age-dependent increases thereafter, apply to the Japanese population. Furthermore, while reports on the frequencies of nodular hyperplasia are found sporadically, there is little data available as to the incidence or size of the lesion by histological type or by location, although such data appear to be significant. Moreover, the frequencies of inflammatory cell infiltration and glandular atrophy are expected to increase with age, but no detailed reports have been published. Recently De Marzo et al. [2] published a report on the association between proliferative inflammatory atrophy (PIA) and cancer, providing additional grounds why looking into the above issue may be worthwhile.

In an attempt to clarify the pathology of the development of prostatic disorders, we investigated age-related changes in prostatic hyperplasia and latent tumors in the Japanese population, and comparatively assessed among age groups prostatic glandular tissue changes such as nodular hyperplasia and lymphocyte infiltration, and prostate histological composition of three components, that is, glandular epithelium, glandular lumen, and stroma.

MATERIALS AND METHODS

Whole-mount step sections of prostatectomy specimens obtained from autopsy at the Department of 2nd Pathology, Mie University, between 1966 and 1993, were used. After being fixed in formalin, the specimens were sectioned perpendicular to the urethra at 3-mm intervals, and then stained using a hematoxylin and eosin (H&E) technique.

The histopathological classification of lymphocyte infiltration was performed as follows according to the classification by True et al. [3]: glandular, periglandular, or stromal for location; mild, moderate, or severe for grade; and focal, multifocal, or diffuse for extent.

Prostate Weight

The relationship between age category and prostate weight was assessed by decade of age group using specimens from 962 males (mean age 64 ± 17 years, range 0–94).

Changes in Prostate Histological Composition by Zone

The prostate histological composition in the transition zone (TZ) and in the peripheral zone (PZ) was compared among the three age groups of 20s, 40s, and 70s. Specimens from 68 subjects with a mean age of 55 ± 19 (range 20–79) years were assessed. The image of each whole section was obtained using a GT-9500 scanner (Epson, Nagano, Japan) for volume estimation. Furthermore, with a DP70 CCD camera (Olympus, Tokyo, Japan), magnified images (100×) were obtained randomly at 10–15 sites per zone at the 0, 2, 4, 8, and 10 o'clock positions in the TZ and at the 2, 4, 6, 8, and 10 o'clock positions in the PZ, mainly in the sections that showed the verumontanum clearly, and were input into the computer (Fig. 1). Quantitative analysis of three components; glandular epithelium, glandular lumen, and stroma, was performed using a computer image analysis system (NIH Image Software). The three-component ratio and volume were compared by age group and by location. Specimens that showed an intensive inflammatory reaction indicative of malignant prostatic lesion or abscess formation were excluded from the assessment.

Prevalence of Nodular Hyperplasia, Calculus, Glandular Dilation, and Lymphocyte Infiltration

The presence or absence of nodular hyperplasia, calculi, glandular dilation, and lymphocyte infiltration in the TZ and in the PZ was assessed by age group (Fig. 2A–D). The specimens were obtained from 102 subjects (mean age 52.9 ± 23.5 years, range 0–93). The presence or absence of the above conditions was evaluated using a BX-50 optical microscope (Olympus, Tokyo, Japan). The largest of the hyperplastic nodules, if present, was measured. Detected hyperplastic nodules were categorized into the glandular, stromal, or mixed type. Glandular dilation of 2 mm or more was considered significant. Specimens that showed an intense inflammatory reaction indicative of malignant prostatic lesion or abscess formation were excluded from the assessment. We summarized the result of lymphocyte infiltration along the classification of Shimomura et al. [4].

Prevalence of Latent Tumors

The prevalence of latent tumors was compared by age group and between the periods up to 1974 inclusive and from 1980 onwards. Specimens from 1985 males (mean age 65 ± 15 years, range 0–96) were assessed. A well-differentiated latent tumor mass was defined as a latent noninfiltrative tumor (LNT) (Fig. 3A), and a moderately to poorly differentiated mass as a latent infiltrative tumor (LIT) (Fig. 3B).

Statistical Processing

Statistical analysis of correlations among age groups was performed using Student's *t*-test (StatView 5.0 software). Statistical significance was taken at $P < 0.05$.

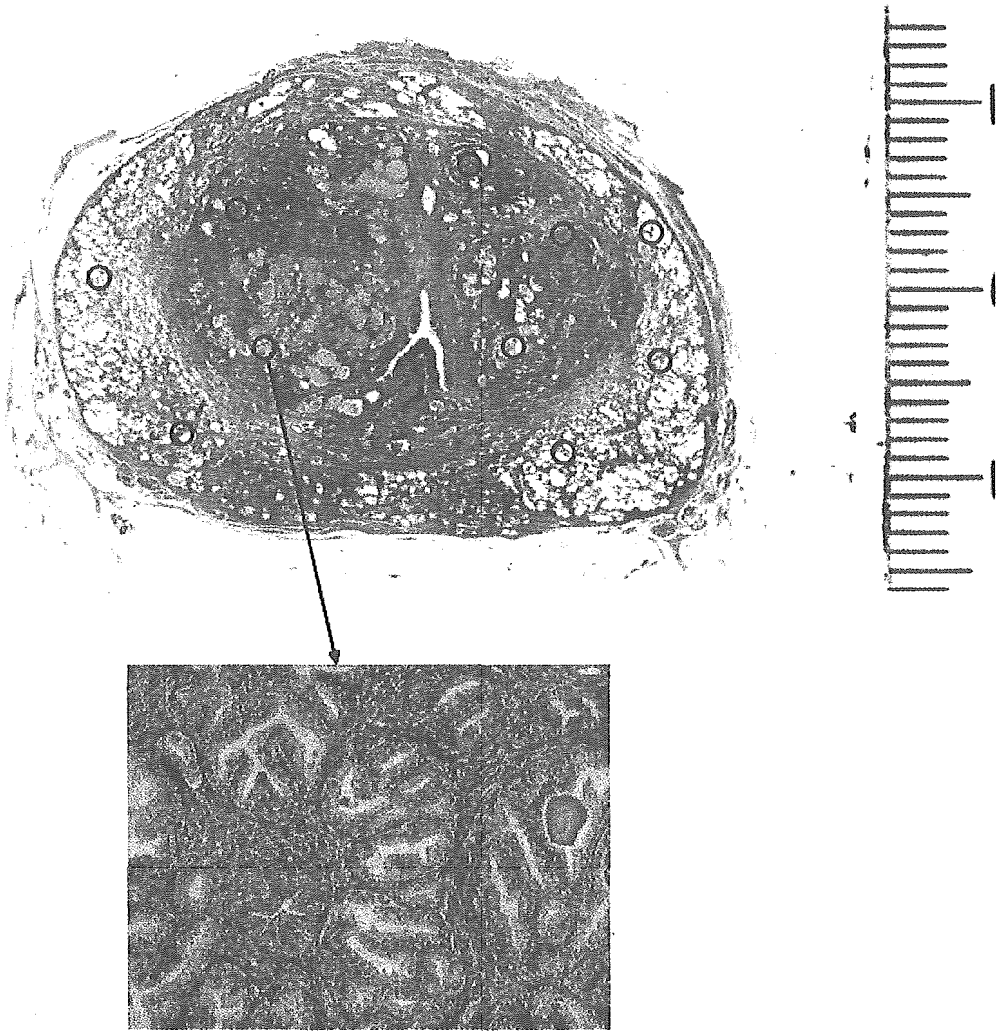

Fig. 1. Sites of the prostate tissues in the transition zone (TZ) and in the peripheral zone (PZ) processed for computer imaging; 10 – 15 images per zone were obtained randomly at the 0, 2, 4, 8 and 10 o'clock positions in the TZ and at the 2, 4, 6, 8, and 10 o'clock positions in the PZ, mainly in the sections that showed the verumontanum clearly. H&E; original magnification 100×.

RESULTS

Relationship Between Age and Prostate Weight (Study 1)

Figure 4 presents the relationship between subject age and prostate weight. A rapid increase in prostate weight ($P < 0.01$) from birth to the 20s was followed by a slow rise with age up to 80. There was no increase observed in the 80s and older groups.

Prostate Volume and Histological Composition in the TZ and PZ (Study 2)

The prostate histological composition and volume in the TZ and in the PZ were compared among three age groups; 20s, 40s, and 70s. Firstly, by-zone changes in the volume of formalin-fixed specimens are presented in Figure 5A. TZ volumes were essentially constant in the 20s and the 40s, while a sharp volume increase ($P < 0.01$) was observed in the 70s compared with the 40s. PZ volumes were highest in the 20s, showing a decreasing trend ($P < 0.05$) with age. Secondly, the volumes of the three components in each zone are shown in Figure 5B–D. In the TZ, the volume of each component was similar between the 20s and 40s, whereas a significant volume increase ($P < 0.01$) was noted for all components in the 70s compared with the 40s. In the PZ, glandular luminal volumes were almost constant throughout all the age categories assessed, while epithelial and stromal volumes decreased significantly ($P < 0.05$) with age after the 20s. TZ versus PZ epithelial proportions in the 20s, 40s, and 70s groups were 8.0%, 8.4%, and 12.5% (TZ) versus 25.1%, 20.2%, and 15.6% (PZ), respectively, showing a

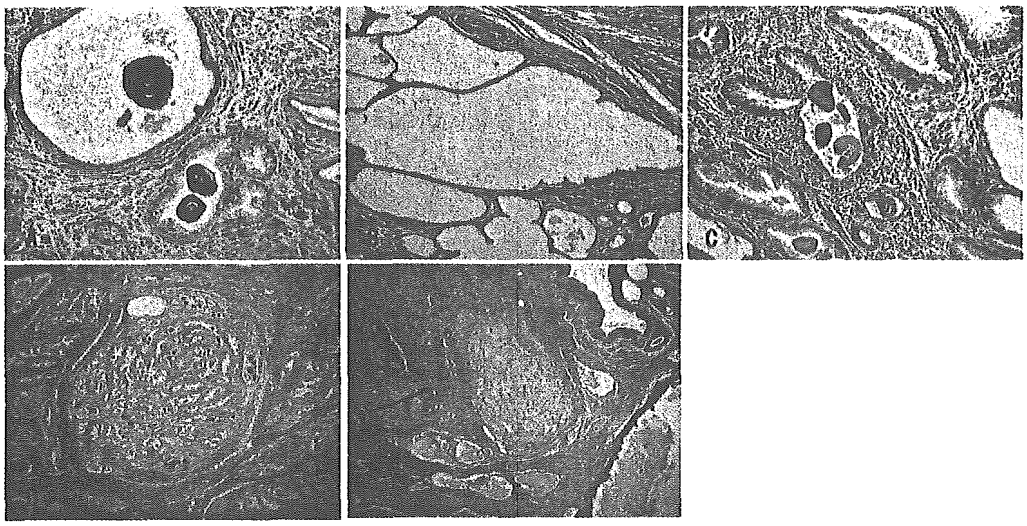

Fig. 2. Histological findings for calculus (A), glandular dilation (B), lymphocyte infiltration (C), and nodular hyperplasia. Hyperplastic nodules were subdivided into glandular (D) and stromal (E) hyperplasia. Glandular dilation of 2 mm or more was considered significant.

tendency consistent with the previous study data, but the differences between zones tended to diminish with advancing age.

Prostate Histological Findings in theTZ and PZ (Study 3)

The occurrence rates of glandular dilation, calculi, and lymphocyte infiltration by zone were compared among age groups. Glandular dilation was detected in each zone in the 30s and older age groups; in the PZ, the occurrence rate increased age-dependently up to the 60s inclusive, but tended to decrease in the 70s and upwards (Fig. 6A). The mean size of dilated gland was comparable in the TZ (2.6 ± 0.6 mm, range 2.0–4.4) and in the PZ (2.8 ± 0.9 mm, range 2.1–6.4), but the occurrence rate tended to be higher in the PZ. Calculi were observed at relatively young ages and tended to increase with advancing age, with high occurrence rates of more than 80% in each zone in the 50s and older groups (Fig. 6B). With regard to lymphocyte infiltration, the occurrence rate in each zone was estimated to increase with age (Fig. 6C). Lymphocyte infiltrates in each zone were divided into subtypes depending on three factors; location, grade, and extent, according to the classification by True et al. [3]. The diffuse-mild-stromal type was most common (30%) in the TZ, and the focal-mild-periglandular type was most common (21%) in the PZ (Table I). Infiltration in the TZ was characterized by a predominance of stromal type, and that in the PZ by infiltration into periglandular tissues.

Frequency of Nodular Hyperplasia (Study 3)

Nodular hyperplasia in the TZ was noted as early as in the 30s age group. The prevalence was 12.5% in the

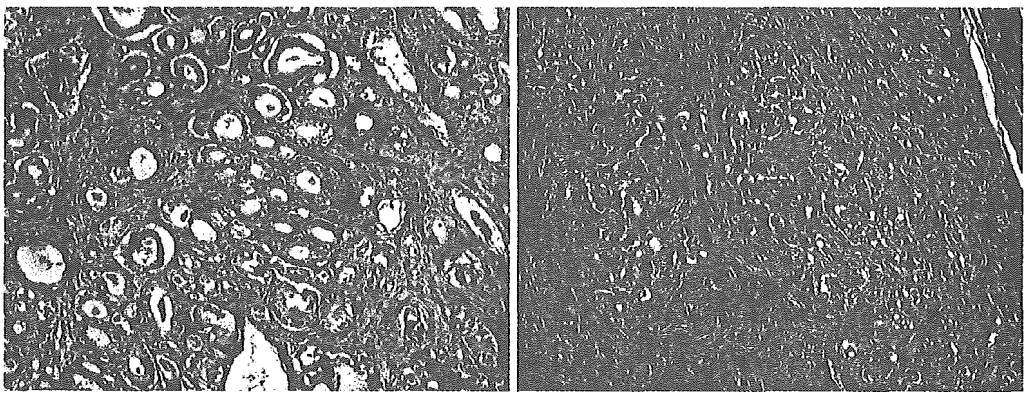

Fig. 3. Histological findings for latent tumors. A well-differentiated mass was defined as an Latent noninfiltrative tumor (LNT) (A) and a moderately to poorly differentiated mass as an Latent infiltrative tumor (LIT) (B). H&E; original magnification 100×.

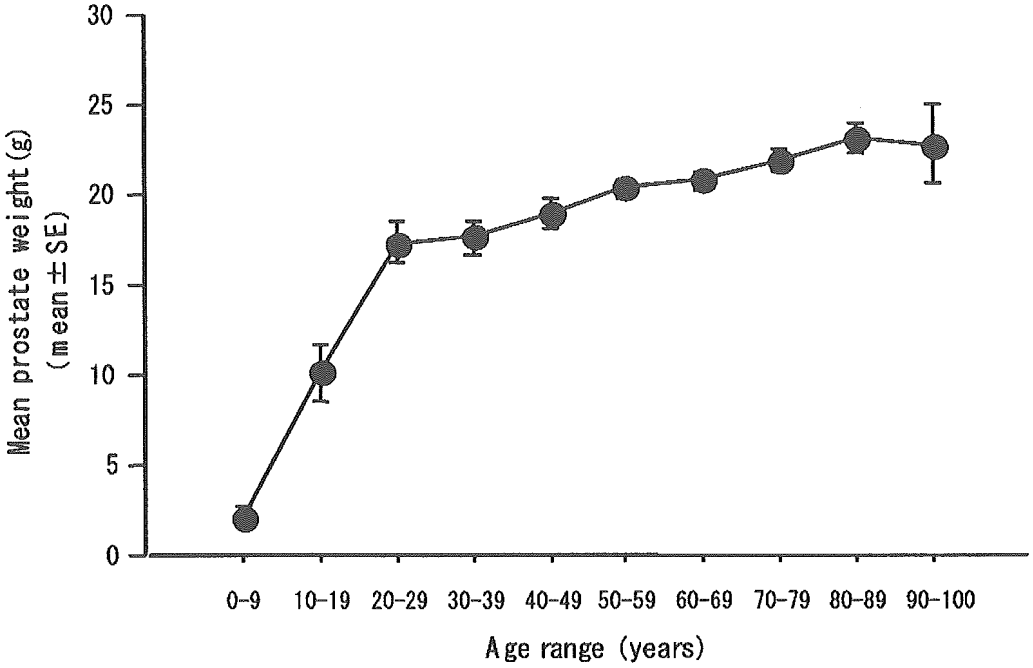

Fig. 4. Distribution of prostate weights by decade of subject age. The specimens were from autopsy of 962 Japanese males.

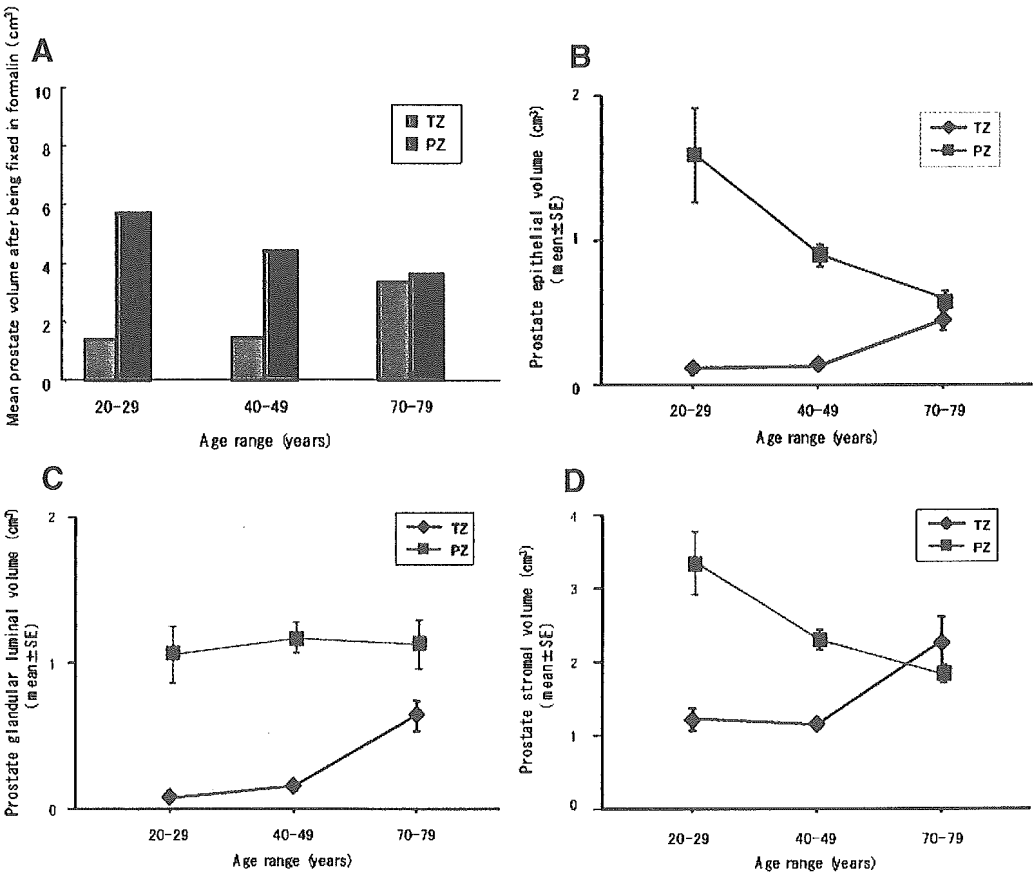

Fig. 5. By-zone volumes of prostate (**A**), epithelial component (**B**), glandular lumen (**C**), and stromal component (**D**). The specimens were from autopsy of 68 Japanese males in their 20s, 40s, and 70s.

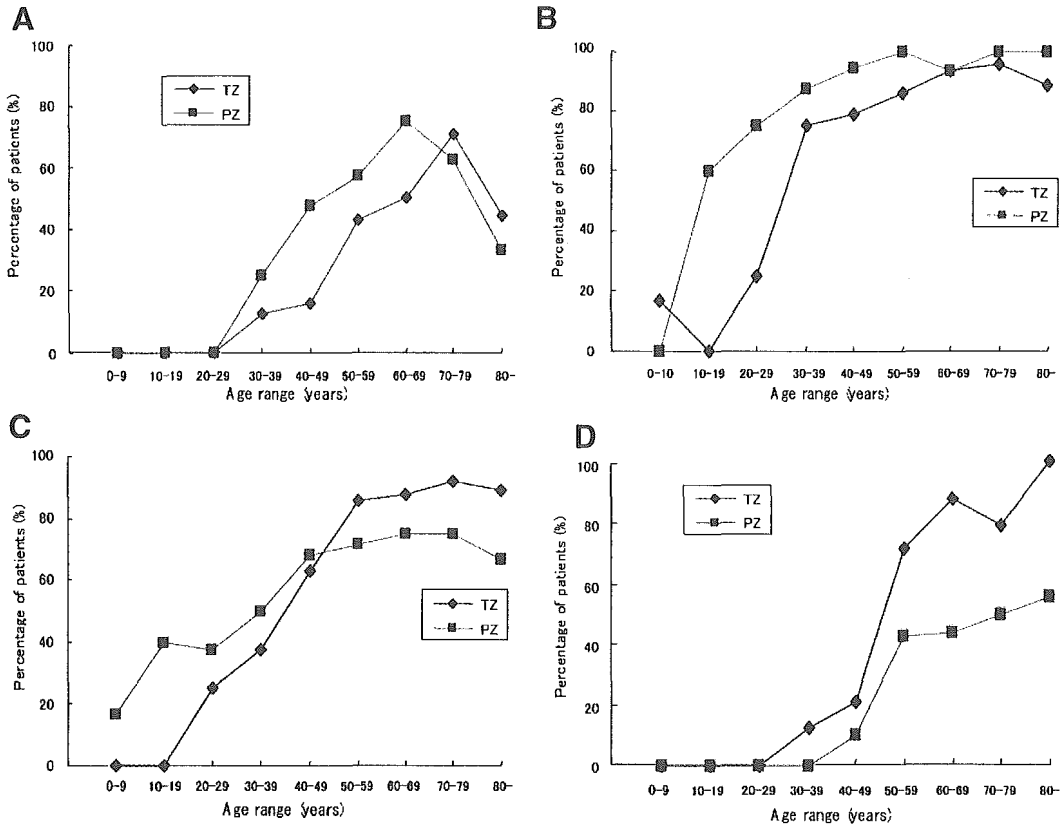

Fig. 6. Frequencies by zone and by decade of age: glandular dilation (**A**), calculi (**B**), lymphocyte infiltration (**C**), and nodular hyperplasia (**D**). The specimens were from autopsy of 102 Japanese males.

TABLE I. Lymphocyte Infiltration Patterns by Transition Zone (TZ) (A) and Peripheral Zone (PZ) (B) Based on the True Classification

		Grade (%)		
Location	Extent	Mild	Moderate	Severe
A (n = 67)				
Glandular	Focal			
	Multifocal			
Periglandular	Focal	3 (4.5)	5 (7.5)	3 (4.5)
	Multifocal	2 (3.0)	5 (7.5)	2 (3.0)
Stromal	Focal	6 (9.0)	3 (4.5)	1 (1.5)
	Multifocal	4 (6.0)	1 (1.5)	3 (4.5)
	Diffuse	17 (25.4)	12 (18.0)	
B (n = 63)				
Glandular	Focal			
	Multifocal		2 (3.2)	
Periglandular	Focal	13 (20.6)	6 (9.5)	1 (1.6)
	Multifocal	8 (12.7)	11 (17.5)	2 (3.2)
Stromal	Focal	4 (6.3)	3 (4.8)	
	Multifocal		3 (4.8)	1 (1.6)
	Diffuse	7 (11.1)	2 (3.2)	

30s group, with a trend towards age-related increase: more than 80% for age 60 or older, and 100% for age 80 or older. Nodular hyperplasia in the PZ was detected as early as in the 40s group. The prevalence was 10.5% in the 40s group, and reached a high rate of over 50% for age 70 and older (Fig. 6D). Hyperplastic nodules in the TZ were characterized by large size, with a mean of 5.0 ± 2.8 mm (range 0.9–12.0), and by stromal (23% of the nodules) as well as glandular composition (Fig. 7A). In the PZ, the mean size was smaller (2.8 ± 1.1 mm, range 1.2–5.6), and almost all hyperplastic nodules were of glandular type (Fig. 7B).

Comparison of Latent Tumor by Age Group (Study 4)

Latent tumors were found as early as in 30s age group, with a prevalence of 5.6% (2 of the 36 specimens). The prevalence tended to increase with age, reaching 43.4% in the 80s. LNT prevalence rates tended to increase up to the 60s inclusive, and remained nearly constant once subjects were over 70. LIT was present in 3.4% of the 40s group, tended to increase with age, and reached a high prevalence rate of 30.7% in the 80s. Comparison between the periods up to 1974 inclusive

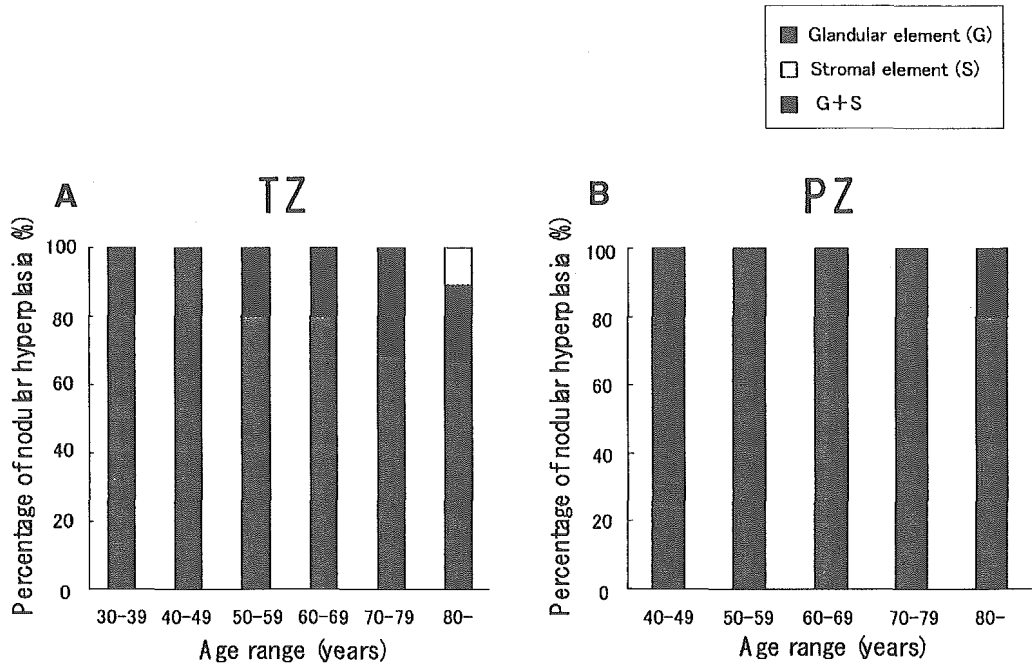

Fig. 7. Frequencies of nodular hyperplasia by histological type in transition zone (TZ) (**A**, n = 39) and in peripheral zone (PZ) (**B**, n = 20).

and from the 1980s onwards revealed a higher prevalence of latent tumors in each decade of age in the later period. In this period, LIT was detected in 5.0% of the 40s group, with the LIT prevalence in each decade of later age being higher in the period from 1980 onwards than in the earlier period (Fig. 8A,B).

DISCUSSION

Regarding prostate weight change with age, Berry et al. [1] reported that weight increased rapidly to about 20 g from birth to age 30, with 3.7% of the prostates from the over 70s age groups weighing more than 100 g, but without BPH, would remain basically constant. The mean prostate weights obtained in our study were lower than those reported by Berry et al. [1], and, while a further trend towards increasing weight was observed by Berry in the 60s and older age groups, in this study, the trend towards increase was only slight in corresponding age groups.

Generally the prostate grows and develops rapidly, mainly in the PZ, during adolescence and starts to shrink in the late 40s, which coincides with frequent adenoma development in the TZ and hyperplasia as a consequence of age-related changes in hormone balance. According to Mori's ultrasonotomographic

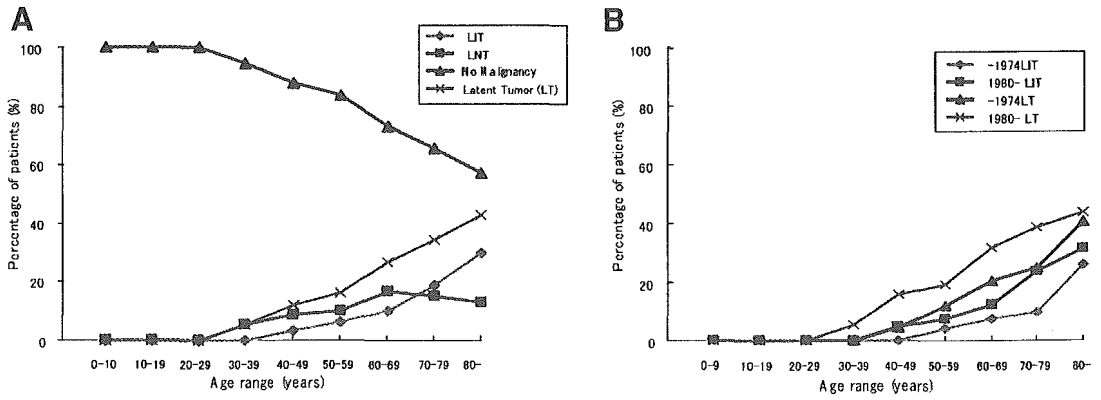

Fig. 8. Frequencies of latent tumors overall and of LIT by decade of age (**A**) and comparison of total latent tumor and LIT frequencies between the period up to 1974 inclusive and that from 1980 onwards (**B**). The specimens were from autopsy of 1815 Japanese males.

assessment study of the normal prostate, prostate weight peaks between ages 21 and 25 years and starts to decrease at 56 years, and this tendency accelerates once the age of 66 years is attained [5]. In the present study, volumes of formalin-fixed TZ specimens remained essentially unchanged in the age range from 20s to 40s and increased rapidly from the 40s to 70s. PZ specimen volumes peaked in the 20s, followed by a tendency to decrease thereafter. These findings indicate that the growth of the PZ is androgen dependent and therefore develops during adolescence, whereas it diminishes in size as androgen levels decrease. On the other hand, it appears that the TZ is estrogen dependent, thus grows in the estrogen-dominant environment resulting from age-related decline in androgen levels.

Aoki et al. [6] evaluated racial differences in cell components of hyperplastic prostates using biopsy specimens obtained from American Caucasians and Japanese, and concluded that Japanese prostates contained fewer stromas and more glandular lumens, based on the ratios of epithelium, glandular lumen, and stroma obtained in those specimens: 12.1%, 3.8%, and 84.2% for the American Caucasians and 15.2%, 7.5%, and 77.4% for the Japanese, respectively. However, there have been only a limited number of reports available on by-zone compositions of prostates of relatively young subjects. Thus we compared TZ and PZ histological compositions and volumes of prostates from subjects in their 20s, 40s, and 70s. In the present study, the TZ composition was found to be 12.5% epithelium, 18.6% glandular lumen, and 68.9% stroma, reflecting a similar tendency to that shown by the data of Aoki et al. [6]. However, the actual percentage of stroma was probably lower than the above figure, because normal prostate specimens were included in our assessment. Comparison of the three components in the TZ among the three age groups revealed similar component proportions and volumes between the 20s and 40s groups, but the percentage ratio of epithelial and the glandular luminal components increased significantly in the 70s compared with the 40s, with a relative decrease in the percentage ratio of stroma. However, in a volume comparison, there was a significant increase in the stroma as well as in the epithelium and in the glandular lumen. While an increase in the stromal component is generally known to be a cause of symptomatic BPH, Ichiyanagi et al. [7] found that the area density of stroma and that of glandular lumen did not differ between the group with bladder outlet obstruction (BOO) and the group without BOO, and that the area density of prostate smooth muscle decreased in the group with BOO. Shapiro et al. [8] reported that the percent area density of prostate smooth muscle in the alpha-blocker responders was 38% greater than in the nonresponders. When determination of the smooth muscle component using biopsy specimens becomes possible, it will probably make it easier to determine the indications for surgery. Furthermore, Lepor et al. [9] and Fukatsu et al. [10] found relationships between serum prostate-specific antigen (PSA) levels and TZ epithelial volumes. In the present study, TZ epithelial volumes increased from the 40s to the 70s, and it is thought that this increase accompanies an increase in PSA level. Next, comparison of the three component proportions and volumes in the PZ among the same age groups revealed nearly constant glandular luminal volumes across all age groups, while epithelial and stromal volumes peaked in the 20s, with significant decreases with age. With regard to prostatic epithelial volume, Lepor et al. [9] and Marks et al. [11] reported that the epithelial component proportion was significantly greater in the PZ than in the TZ. In the present study, the TZ versus PZ epithelial proportions in the 20s, 40s, and 70s groups showed a tendency consistent with the previous study data, but the differences between zones tended to diminish with advancing age.

No detailed reports have been published on prostate glandular dilation. In the present study, dilated glandular lumens in the TZ and in the PZ were compared among the age groups. Dilation was found in each zone in the 30s and older groups, with a trend towards high prevalence in the PZ in the early decades of life. These observations indicate that in the PZ, where glandular secretion becomes active during adolescence, the glandular lumens may be obstructed, resulting in high occurrence rates of glandular dilation. However, the prevalence of glandular dilation tended to decrease in the over 70s groups, which may be attributable to glandular atrophy following dilation. In addition, it was suggested that post-glandular obstruction PSA leakage into the bloodstream could possibly lead to an increase in serum PSA levels. There is a paucity of prostate calculus reports also. Among published reports, those are by Klimas et al. and by Sondergaard et al. Klimas et al. [12] found that prostate calculi were infrequent in the 40s and younger groups and were commonly seen in the 50s and older groups, and identified the cause of calculi as calcified amyloid deposition secondary to prostatic fluid obstruction and stagnation. Sondergaard et al. [13] reported that calculi were present in 99% of the 300 prostates studied, their number and size increasing with age. In the present study, a calculus of unidentified size was detected in the TZ of one (16.6%) of the six prostates in males from the first decade of age. PZ calculi, as compared with TZ, were seen at higher rates from relatively early age, with a trend towards increasing prevalence with age.

Regarding lymphocyte infiltration in the prostate, True et al. [3] classified prostate biopsy specimens from patients with chronic prostatitis or chronic pelvic pain syndrome into histopathological subtypes. To our knowledge, there have been no documented classifications of whole-mount sections of specimens by age group. In the present study, lymphocyte infiltration was detected in the PZ of one (16.7%) of the six specimens, and in both zones in samples from the 20s and older groups, showing an increasing tendency with age. Histopathological subtype categorization revealed that stromal infiltration was characteristic of the TZ, as evidenced by lymphocyte infiltration involving stromal nodules in this zone, and infiltration into periglandular tissues was characteristic of the PZ.

Berry et al. [1] reported the presence of nodular hyperplasia in only 8% of the prostates in subjects in their 30s but in 50% in the 50s age group. Our findings were consistent with the above data; in the present study, the prevalence of nodular hyperplasia in the TZ was 16.7% in the 30s age group, tended to increase with age, and was more than 70% in the 50s and older groups. Regarding nodular hyperplasia in the PZ, Oyen et al. [14] reported a prevalence of 5.5% for their biopsy samples, and Van de Voorde et al. [15] reported a prevalence of 18.5% for their radical prostatectomy specimens. However, there is little published data for hyperplasia by age group. In the present study, we detected PZ nodular hyperplasia in 10.5% of the specimens from the 40s age group and in over 50% of specimens from the over 70s groups. Hyperplastic nodules in the TZ were characterized by large size, with the mean of 5.0 ± 2.8 (range 0.9–12.0) mm, and by stromal (23%) as well as glandular composition. In the PZ, the mean size was smaller (2.8 ± 1.1 mm, range 1.2–5.6), and almost all hyperplastic nodules were of glandular type. Van de Voorde et al. [15] also reported that half of the hyperplastic nodules in the PZ were unifocal, that the mean diameter of PZ nodules was small at 4 ± 1.3 mm, and that no pure stromal nodules without glands were seen. Our findings were consistent with those observations. As a possible developmental mechanism, Pradhan et al. [16] reported that nodular hyperplasia originated as an early stromal nodule usually by the side of the urethra, stimulating the duct in its vicinity to proliferate. With respect to nodular hyperplasia in the PZ, a zone-specific mechanism of development appears to exist.

The prevalence of latent tumors found at autopsy varies widely from 4.3% to 46% depending on reports. This may be attributed to differences in age and/or ethnic background of the subjects, or to the report retrieval system. Regarding latent tumor frequency in young populations, Sakr et al. [17] identified small foci of histological cancer in 27% of the subjects in their 30s. It is generally accepted that latent tumors are present in individuals as early as in the fourth decade of life. The present study results support this view. As opposed to no latent cancer in the specimens from subjects aged less than 30 years, we found latent tumors in two (5.6%) of the 36 specimens from subjects in the 31 to 40 years age group, and the frequency tended to increase with age. Assessment of these tumors in terms of degree of histopathological differentiation showed that the age-dependent increase in the frequency of latent tumors overall may reflect the trend of LIT increase with age. In general, the prevalence rates of prostate (including both clinical and latent) tumors are higher in Western countries than in Asian countries. Among Japanese, Caucasian-Americans and African-Americans, the prevalence rates of latent tumors are highest in African-Americans, followed by Caucasian-Americans, and then Japanese with advancing age overall. Although there is an over ten times higher rate of clinical tumors in African-Americans as compared to Japanese, the difference of latent tumors is approximately two times, suggesting the developmental differences of prostate tumor among three population groups [18]. Association with the increasing adoption of the Western diet in Japan was also assessed by comparing the latent tumor frequency for the period from 1966 to 1974 with the period from 1980 to 1993. The frequency of latent tumors overall increased from about 20% to about 30% from the first to the second periods, with the occurrence rates of LIT being approximately 1.8-times higher in the later period. Given the rapid spread in recent years of prostate cancer screening employing serum PSA, the frequency of latent tumors is estimated to decrease as the clinical cancer detection rate rises.

REFERENCES

1. Berry SJ, Coffey DS, Walsh PC, Ewing LL. The development of human benign prostatic hyperplasia with age. J Urol 1984; 132:474–479.
2. De Marzo AM, Marchi VL, Epstein JI, Nelson WG. Proliferative inflammatory atrophy of the prostate: Implications for prostatic carcinogenesis. Am J Pathol 1999;155:1985–1992.
3. True LD, Berger RE, Rothman I, Ross SO, Krieger JN. Prostate histopathology and the chronic prostatitis/chronic pelvic pain syndrome: A prospective biopsy study. J Urol 1999;162:2014–2018.
4. Shimomura T, Kiyota H, Takahashi H, Madarame J, Kimura T, Onodera S. Prostate histopathology of NIH category IV prostatitis detected by sextant prostate needle biopsy from the patients with high prostatic specific antigen. Kansenshogaku Zasshi 2003;77:611–617 (in Japanese).
5. Mori Y. Measurement of the normal prostate size by means of transrectal ultrasonotomography. Jpn J Urol 1982;73:767–781 (in Japanese).

6. Aoki Y, Arai Y, Maeda H, Okubo K, Shinohara K. Racial differences in cellular composition of benign prostatic hyperplasia. Prostate 2001;49:243–250.
7. Ichiyanagi O, Sasagawa I, Ishigooka M, Suzuki Y, Nakada T. Morphometric analysis of symptomatic benign prostatic hyperplasia with and without bladder outlet obstruction. Urol Res 2000;28:29–32.
8. Shapiro E, Hartanto V, Lepor H. The response to alpha blockade in benign prostatic hyperplasia is related to the percent area density of prostate smooth muscle. Prostate 1992;21:297–307.
9. Lepor H, Wang B, Shapiro E. Relationship between prostatic epithelial volume and serum prostate-specific antigen levels. Urolpgy 1994;44:199–205.
10. Fukatsu A, Ono Y, Ito M, Yoshino Y, Hattori R, Gotou M, Ohshima S. Relationship between serum prostate-specific antigen and calculated epithelial volume. Urology 2003;61: 370–374.
11. Marks LS, Treiger B, Dorey FJ, Fu YS, deKernion JB. Morphometry of the prostate: I. Distribution of tissue components in hyperplastic glands. Urology 1994;44:486–492.
12. Klimas R, Bennett B, Gardner WA Jr. Prostatic calculi: A review. Prostate 1985;7:91–96.
13. Sondergaard G, Vetner M, Christensen PO. Prostatic calculi. Acta Pathol microbiol immunol scand [A] 1987;95:141–145.
14. Oyen RH, Van de Voorde WM, Van Poppel HP, Brys PP, Ameye FE, Franssens YM, Baert AL, Baert LV. Benign prostatic nodules that originate in the peripheral zone of the prostate gland. Radiology 1993;189:707–711.
15. Van de Voorde WM, Oyen RH, Van Poppel HP, Wouters K, Baert LV, Lauweryns JM. Peripherally localized benign hyperplastic nodules of the prostate. Mod Pathol 1995;8:46–50.
16. Pradhan BK, Chandra K. Morphogenesis of nodular hyperplasia—prostate. J Urol 1975;113:210–213.
17. Sakr WA, Haas GP, Cassin BF, Pontes JE, Crissman JD. The frequency of carcinoma and intraepithelial neoplasia of the prostate in young male patients. J Urol 1993;150:379–385.
18. Shiraishi T, Watanabe M, Matsuura H, Kusano I, Yatani R, Stemmermann GN. The frequency of latent prostatic carcinoma in young males: The Japanese experience. In Vivo 1994;8: 445–447.

Neurochemical Research, Vol. 30, No. 1, January 2005 (© 2005), pp. 75–81
DOI: 10.1007/s11064-004-9688-1

Age-related Decline of Brain Monoamines in Mice is Reversed to Young Level by Japanese Herbal Medicine

A. Tsunemi,[1] M. Utsuyama,[1,2] B. K. H. Seidler,[1] S. Kobayashi,[2] and K. Hirokawa[1,3]

(Accepted September 30, 2004)

Young (3-month-old) and aged mice (18-month-old) were fed a diet containing Japanese herbal medicine (TJ-41 or TJ-48) for 5 months, and the effect of the herbal medicines were examined in terms of levels of monoamines and their metabolites in the brain of young and aged mice. In the aged mice, the levels of norepinepherine, serotonin and their metabolites in the brain were decreased in the cortex, hippocampus and hypothalamus. Feeding of diet containing TJ-48, but not TJ-41, enhanced the levels of some monoamines and their metabolites in the brains of aged mice, comparable to those of young mice. The results indicated that the improvement of levels of monoamines by Japanese herbal medicine was observed only in the aged mice, not in the young mice. The data have suggested the importance of the aged animals to see the effect of medicine on the functions of organs or systems.

KEY WORDS: Aged mice; brain monoamines; Japanese herbal medicine; restoration.

INTRODUCTION

Physiological functions generally decrease with age and the accompanying alteration of behavior, causing many disorders in the elderly (1). Therefore, restoration of the physiological functions of the elderly has been desire for many years. We have tried various methods to restore immunological functions using animal models (2). Among various methods, Japanese herbal medicines are most easily applicable to humans. Actually, a group of Japanese herbal medicines, the so-called 'Kampo-hozai', has been used for the improvement of the physiological conditions of frail patients suffering from various diseases. Among the various Kampo-hozais (Japanese herbal medicines), we reported that Hochu-ekki-to (TJ-41) and Juzen-taiho-to (TJ-48) are effective in the restoration of immune functions of aged mice (3). Since the immune system is functionally closely related to the nervous system (4,5), we speculated that these Kampo-hozais might also influence brain function. Therefore, in this report, we examined the effects of these Kampo-hozais on the concentration of various monoamines in the brain of young and old mice.

[1] Department of Pathology and Immunology, Tokyo Medical & Dental University Graduate School.
[2] Neuronal Function Research Group, Tokyo Metropolitan Institute of Gerontology.
[3] Address reprint requests to: K. Hirokawa M.D., Ph.D., Department of Pathology and Immunology, Tokyo Medical & Dental University Graduate School, 1-5-45, Yushima, Bunkyo-ku, Tokyo 113-8519, Japan. Tel: +81-3-5803-5173; Fax: +81-3-5803-0123; E-mail: hirokawa.pth2@tmd.ac.jp

MATERIALS AND METHODS

Mice. C57BL/6 male mice were purchased from SLC (Shizuoka, Japan). The young mice were 3 months old and the aged mice were 18 months old. The aged mice were maintained in a SPF colony of Tokyo Metropolitan Institute of Gerontology. The mice were maintained at 12-h light 12-h dark cycle (light on at 08:00). They had free access to food and water.

Japanese Herbal Medicine (Kampo-hozai). Hochu-ekki-to (TJ-41) was prepared as a spray-dried powder of hot-water extract obtained from ten medical plants in the ratio of Astragali Radix (4.0), Atractylodis Lanceae Rhizoma (4.0), Ginseng Radix (4.0),

Angelicae Radix (3.0), Bupleuri Radix (2.0), Zizyphi Fructus (2.0), Auranti Nobilis Pericarpium (2.0), Glycyrrhizae Radix (1.5), Cimicifugae Rhizoma (1.0) and Gingiberis Rhizoma (0.5). Juzen-taiho-to (TJ-48) was prepared in the same way from 10 medical plants in the ratio of Astragali Radix (3.0), Cinamomi Cortex (3.0), Rehmanniae Radix (3.0), Paeoniae Radix (3.0), Cnidii Rhizoma (3.0), Angelicae Radix (3.0), Ginseng Radix (3.0), Hoelen (3.0), Glycyrrhizae Radix (1.5) and Atractylodis Lanceae Rhizoma (3.0).

Administration Protocol of Kampo-hozai. The regular diet, CE-2 (Clea, Japan), was mixed with 1.6% of Hochu-ekki-to (TJ-41 diet) or Juzen-taiho-to (TJ-48 diet). The young and aged mice were separated into three groups and given either regular diet (control), TJ-41 diet or TJ48 diet for 5 months. The amount of diet taken per mouse was approximately 3.6 g/day in both young and aged mice. Accordingly, the amount of Kampo-hozai taken per mouse for 5 months was estimated at approximately 8 g in total. Six and seven mice were used for control and experimental groups, respectively.

Determination of Monoamines and their Metabolites in the Brain. All mice were sacrificed at 5 months after the start of the diet containing Kampo-hozai and the brain was used for determination of monoamines and their metabolites, as reported previously (6). The age of the young mice was 8 months and that of the aged mice, 23 months at the time of determination of monoamines. The frontal cortex, hippocampus and hypothalamus were dissected on ice, according to the method of dissection procedures for preparation of slice cultures (7), rapidly frozen in liquid nitrogen and stored at −80°C until use. The frozen tissue was homogenized in 0.2 M perchloric acid (PCA) containing 100 μM EDTA–2Na and 50 ng Internal standard (Isoproterenol). After centrifugation (10,000 rpm, 15 min, 0°C), a part of the supernatant was used for protein assay and the other 10 μl aliquot was adjusted to pH 3 with 2 M sodium acetate and injected into a high-performance liquid chromatography (HPLC) system with an electrochemical detector for the determination of norepinephrine (NE), normetanephrine (NM), 4-hydroxy-3-methoxyphenylglycol (MHPG), dopamine (DA), 3,4-dihydroxyphenylacetic acid (DOPAC), 4-hydroxy-3-methoxyphenylacetic acid (HVA), 3-methoxytyramine (3-MT), serotonin (5-HT), and 5-hydroxyindole-3-acetic acid (5-HIAA). The electrode potential was set at 750 mV vs. an Ag/AgCl reference electrode. The mobile phase used for the assay was 0.1 M citrate-acetic acid buffer containing 17% methanol and 190 mg/L SOS (1-Octanesulfonic acid sodium salt), pH 3.5, 25°C. The flow rate was 0.5 ml/min. The HPLC system consisted of a reverse-phase column (Eicompak SC-5ODS), a pre-column (PREPACK) and an electrochemical detector ECD-300 (300 Series, Eicom Co., Kyoto, Japan). The quantity of protein in the tissue sample was measured by a protein assay kit. The amount of monoamines and metabolites was shown as the ratio to total protein (pg/ng).

Statistics. Data were presented as mean ± SEM, calculated from six or seven mice for each group. Results were analyzed using student's *t*-test.

RESULTS

Age Difference in the Content of Various Monoamines and their Metabolites

At 5 months after the onset of the experiment, all mice were sacrificed, and the brains and spleens were used for examination. Table I summarizes the content of various monoamines and their metabolites in the cortex, hippocampus and hypothalamus in the young and aged mice. Among the three loci, the hypothalamus contained higher levels of norepinepherine (NE), serotonin (5-HT) and dopamine (DA) as compared with those of the cortex and hippocampus. First, we examined the age change of monoamines and their metabolites in these three loci.

(a) The cortex showed a significant age-related decline in norepinepherine and its metabolites: NE (10.21 ± 0.68 vs. 7.03 ± 0.75), NM (1.70 ± 0.20 vs. 0.97 ± 0.15), and MHPG (2.63 ± 0.26 vs. 1.35 ± 0.15). Serotonin showed a trend of decline (8.30 ± 0.84 vs. 6.38 ± 0.51), but its metabolite, 5-HIAA, showed a significant decline with age (7.77 ± 1.01 vs. 4.82 ± 0.71). Dopamine and its metabolites showed a trend of decline with age.

(b) The hippocampus showed a significant decline in serotonin (5-HT) (7.41 ± 0.54 vs. 5.07 ± 0.72) and 5-HIAA (13.99 ± 1.15 vs. 9.11 ± 0.88). Norepinepherine (NE) and its metabolite (NM) showed a trend of decline with age, and the level of MHPG significantly decreased with age (2.50 ± 0.25 vs. 1.10 ± 0.12). Dopamine and its metabolites showed a trend of decline with age.

(c) The hypothalamus showed a significant decline in norepinephrine (NE) and serotonin (5-HT), and their metabolites: NE (15.26 ± 1.76 vs. 8.73 ± 0.84), NM (0.56 ± 0.05 vs. 0.37 ± 0.03), MHPG (4.42 ± 0.83 vs. 1.69 ± 0.18), 5-HT (13.30 ± 2.25 vs. 6.06 ± 0.83), 5-HIAA (15.57 ± 0.09 vs. 6.85 ± 0.57). Dopamine (DA) showed a trend of decline, but a significant decline was observed in its metabolites HVA (6.03 ± 1.12 vs. 2.55 ± 0.33) and 3-MT (1.25 ± 0.36 vs. 0.39 ± 0.12).

Effect of Kampo-hozai on the Levels of Monoamines and their Metabolites in the Brain

Next, we compared the levels of monoamines and their metabolites between the control mice and those given TJ-41 and TJ-48.

(a) Cortex (Fig. 1). The low level of NE in the aged mice was significantly enhanced in the mice given TJ-48 (7.03 ± 0.75 vs. 10.65 ± 1.23), but not TJ-41 (7.03 ± 0.75 vs. 7.68 ± 0.71). Similar enhancement was observed with the metabolites of NE, NM (0.97 ± 0.15 vs. 2.02 ± 0.33) and MHPG (1.35 ± 0.15 vs. 3.14 ± 0.37). The low content of

Table 1. Concentration of Monoamines and their Metabolites in the Brain

		Dopamine and metabolites				Norepinephrine and metabolites			Serotonin and metabolites	
Cortex		DA (Dopamine)	DOPAC	HVA	3-MT	NE(Norepinephrine)	NM	MHPG	5-HT (Serotonin)	5-HIAA
Young	Cont	4.94 ± 2.71	1.82 ± 0.51	3.98 ± 0.98	0.70 ± 0.19	10.21 ± 0.68	1.70 ± 0.20	2.63 ± 0.26	8.30 ± 0.84	7.77 ± 1.01
	TJ-41	11.79 ± 5.10	2.20 ± 0.76	3.73 ± 1.05	1.18 ± 0.33	10.04 ± 0.69 #	1.64 ± 0.10 #	2.87 ± 0.59 *	9.83 ± 1.25	5.61 ± 1.21 * #
	TJ-48	2.86 ± 1.85	0.92 ± 0.19	2.53 ± 0.43	0.65 ± 0.12	9.98 ± 0.67	2.20 ± 0.24	2.49 ± 0.22	9.54 ± 0.84	3.72 ± 0.30
Aged	Cont	2.18 ± 0.79	1.00 ± 0.19	2.23 ± 0.34	0.44 ± 0.05	7.03 ± 0.75	0.97 ± 0.15	1.35 ± 0.15	6.38 ± 0.51 *	4.82 ± 0.71
	TJ-41	1.03 ± 0.10	0.90 ± 0.11	1.89 ± 0.17	0.44 ± 0.07 #	7.68 ± 0.71 #	1.42 ± 0.14 #	1.74 ± 0.23	6.56 ± 0.93	5.02 ± 0.37
	TJ-48	10.08 ± 4.60	1.36 ± 0.30	3.32 ± 0.71	1.01 ± 0.25	10.65 ± 1.23	2.02 ± 0.33	2.14 ± 0.37	10.23 ± 0.96	4.44 ± 0.65
Hippocampus										
Young	Cont	12.44 ± 11.66	2.24 ± 1.81	3.72 ± 2.61	1.20 ± 0.83	8.30 ± 0.91	0.82 ± 0.13	2.50 ± 0.25	7.41 ± 0.54	13.99 ± 1.15 *
	TJ-41	25.19 ± 24.73	4.44 ± 4.01	3.15 ± 2.18	2.45 ± 2.01	6.68 ± 1.35	1.10 ± 0.21	1.79 ± 0.21 *	6.11 ± 0.70 #	7.78 ± 0.82 *
	TJ-48	0.35 ± 0.06	0.28 ± 0.03	0.86 ± 0.08	0.32 ± 0.03	8.70 ± 0.58	0.89 ± 0.13	2.27 ± 0.25	8.01 ± 0.56	9.70 ± 0.88 *
Aged	Cont	0.36 ± 0.04	0.25 ± 0.03	0.61 ± 0.07	0.31 ± 0.04	5.88 ± 0.67	0.76 ± 0.08	1.10 ± 0.12	5.07 ± 0.72	9.11 ± 0.88
	TJ-41	0.37 ± 0.03	0.33 ± 0.02	0.72 ± 0.04	0.37 ± 0.03	6.33 ± 0.41 #	0.89 ± 0.08 #	1.23 ± 0.15 *	5.24 ± 0.52 *	9.34 ± 0.73
	TJ-48	0.32 ± 0.04	0.30 ± 0.03	0.83 ± 0.07	0.45 ± 0.08	8.17 ± 0.62	1.14 ± 0.12	1.97 ± 0.17	9.06 ± 0.80	12.16 ± 1.42
Hypothalamus										
Young	Cont	13.62 ± 4.38	4.50 ± 1.30	6.03 ± 1.12	1.25 ± 0.36	15.26 ± 1.76	0.56 ± 0.05	4.42 ± 0.83	13.30 ± 2.25	15.57 ± 3.09
	TJ-41	20.01 ± 7.83	3.93 ± 0.87	6.14 ± 1.31 #	4.85 ± 2.71 #	15.02 ± 2.61 *	1.76 ± 0.76 *	3.75 ± 0.71 *	13.90 ± 2.64 #	9.42 ± 1.83 #
	TJ-48	10.40 ± 2.65	2.76 ± 0.42	4.71 ± 0.82	0.94 ± 0.25	16.25 ± 1.55	0.75 ± 0.09	3.30 ± 0.51	13.13 ± 1.54	9.36 ± 1.24
Aged	Cont	4.88 ± 1.18	1.68 ± 0.28	2.55 ± 0.33	0.39 ± 0.12	8.73 ± 0.84	0.37 ± 0.03	1.69 ± 0.18	6.06 ± 0.83	6.85 ± 0.56
	TJ-41	7.03 ± 2.05	2.23 ± 0.35	3.48 ± 0.51	0.59 ± 0.14	11.41 ± 1.68 #	0.50 ± 0.03 *	2.77 ± 0.50 *	9.25 ± 1.53 *	8.38 ± 0.41
	TJ-48	5.20 ± 0.56	1.66 ± 0.13	3.43 ± 0.37	0.46 ± 0.06	12.84 ± 1.10	0.64 ± 0.04	2.83 ± 0.16	10.68 ± 0.57	7.94 ± 0.48

Values are shown as concentration per total protein assessed (pg/ng). All data are the mean ± one standard error of the mean (SEM), calculated from 8 or six or seven mice for each group. $^{\#}P<0.05$. $^{*}P<0.05$ in comparison with control. DOPAC: 3,4-dihydroxyphenylacetic acid. HVA: homovanillic acid. 3-MT: 3-methoxytylamine. NM: Normethanephrine. MHPG: hydroxymethophenylglycol piperzinesalt. 5-HIAA: 5-hydroxyindole-3-acetic acid. Metabolic pathways of brain monoamines are show